derivatives[1,2] and poly(*n*-hexyl isocyanate).[29]

Acknowledgment. We express our appreciation to Prof. G. Torri for the NMR determinations. This investigation has been supported by the Italian Research Council through its "Chimica Fine e Secondaria" project.

Registry No. CA, 9004-35-7; DMAc, 127-19-5.

References and Notes

(1) Conio, G.; Bianchi, E.; Ciferri, A.; Tealdi, A.; Aden, M. A. *Macromolecules* **1983**, *16*, 1264.
(2) Aden, M. A.; Bianchi, E.; Ciferri, A.; Conio, G.; Tealdi, A. *Ibid.* **1984**, *17*, 2010.
(3) Terbojevich, M.; Cosani, A.; Conio, G.; Ciferri, A.; Bianchi, E. *Ibid.* **1985**, *18*, 640.
(4) Bianchi, E.; Ciferri, A.; Conio, G.; Cosani, A.; Terbojevich, M. *Ibid.* **1985**, *18*, 646.
(5) Meeten, G. H.; Navard, P. *Polymer* **1983**, *24*, 815.
(6) Marsano, E.; Bianchi, E.; Ciferri, A. *Macromolecules* **1984**, *17*, 2886.
(7) Dayan, S.; Maissa, P.; Vellutini, P.; Sixou, P. *J. Polym. Sci., Polym. Lett. Ed.* **1982**, *20*, 33.
(8) Flory, P. J. *Proc. R. Soc. London, A.* **1956**, *234*, 60.
(9) Flory, P. J. *Adv. Polym. Sci.* **1984**, *59*, 1.
(10) Patel, D. L.; Gilbert, R. D. *J. Polym. Sci., Polym. Phys. Ed.* **1983**, *21*, 1079.
(11) Kamide, K.; Miyazaki, Y.; Abe, T. *Polym. J. (Tokyo)* **1979**, *11*, 523. Kamide, K.; Terakawa, T.; Miazaki, Y. *Ibid.* **1979**, *11*, 285.
(12) Kamide, K.; Saito, M. *Ibid.* **1982**, *14*, 517.
(13) Goodlett, V. W.; Dougherty, J. T.; Patton, H. W. *J. Polym. Sci., Polym. Chem. Ed.* **1971**, *9*, 155.
(14) ASTM D-871-56 (ASTM Standards 1958, Part 8 Lacquers and Lacquer Materials, p 460).
(15) Kamide, K.; Saito, M.; Abe, T. *Polym. J. (Tokyo)* **1981**, *13*, 421.
(16) Saito, M. *Ibid.* **1983**, *15*, 249.
(17) Yamakawa, H.; Fujii, M. *Macromolecules* **1974**, *7*, 128.
(18) Brant, D. A.; Goebel, K. D. *Ibid.* **1972**, *5*, 536.
(19) Marchessault, R. M.; Sarko, A. *Adv. Carbohydr. Chem.* **1967**, *22*, 421.
(20) Panar, M.; Wilcok, O. B. Ger. Offen. 2705382, Aug 11, 1977. Fr. Demande 77, 3473, 1977 (to the Du Pont Co.).
(21) Saito, M. *Polym. J. (Tokyo)* **1983**, *15*, 213.
(22) Kirkwood, J.; Riseman, J. R. *J. Chem. Phys.* **1948**, *16*, 565.
(23) Papkov, S. *Contemp. Top. Polym. Sci.* **1977**, *2*.
(24) Balbi, C.; Bianchi, E.; Ciferri, A.; Tealdi, A.; Krigbaum, W. R. *J. Polym. Sci., Polym. Phys. Ed.* **1980**, *18*, 2037.
(25) Ciferri, A.; Krigbaum, W. R. *Mol. Cryst. Liq. Cryst.* **1981**, *69*, 273.
(26) Flory, P. J. *Macromolecules* **1978**, *11*, 1141.
(27) Khokhlov, A. R. Semenov, A. N. *Physica A* **1982**, *112A*, 605.
(28) Warner, M.; Flory, P. J. *J. Chem. Phys.* **1980**, *73*, 6327.
(29) Krigbaum, W. R.; Hakemi, M.; Ciferri, A.; Conio, G. *Macromolecules* **1985**, *18*, 973.
(30) Ronca, G.; Yoon, D. Y. *J. Chem. Phys.* **1985**, *83*, 373.

Phase Structure of Lamellar Crystalline Polyethylene by Solid-State High-Resolution ^{13}C NMR: Detection of the Crystalline–Amorphous Interphase

Ryozo Kitamaru,* Fumitaka Horii, and Kouichi Murayama

Institute for Chemical Research, Kyoto University, Uji City, Kyoto 611, Japan.
Received June 5, 1985

ABSTRACT: The phase structure of lamellar crystalline polyethylene is investigated in detail by high-resolution solid-state ^{13}C NMR, utilizing different pulse sequences for spectrum detections. It is concluded that samples crystallized from the melt consist of the lamellar crystalline phase, a crystalline–amorphous interphase, and an isotropic amorphous phase, whereas samples crystallized from dilute solution consist of the lamellar crystalline phase and a noncrystalline overlayer. These component phases are explicitly characterized in terms of the chemical shift and the spin–lattice and spin–spin relaxation times.

Introduction

Lamellar crystalline polyethylene contains a noncrystalline part to some extent, whether it is crystallized from the melt or from dilute solution. A question arises as to whether this noncrystalline content is in a disordered amorphous state or in any particular ordered state due to the coexistence of lamellar crystallites. This problem has been extensively studied for several decades. It has been found by ^1H broad-line NMR investigations that samples crystallized from the melt (hereafter referred to as bulk crystals) generally consist of three regions: the crystalline region with molecular chains oriented perpendicular to the wide faces of the lamella, the noncrystalline interfacial region with limited molecular mobility, and the noncrystalline interzonal region with liquidlike molecular mobility.[1-5] Polyethylene samples crystallized from dilute solution (hereafter referred to as solution crystals) consist of lamellar crystals and noncrystalline overlayers with a negligibly small amount of noncrystalline interzonal material with pronounced molecular mobility.[2-4]

It has also been found that both bulk crystals and solution crystals contain a noncrystalline part that can be detected by ^1H scalar-decoupled ^{13}C NMR.[6,7] The ^{13}C spin–lattice relaxation time T_{1C} is almost the same at room temperature for the two series of samples, whereas the spin–spin relaxation time T_{2C} of the solution crystals is much shorter than that of the bulk crystals. Therefore, one can assume that the noncrystalline overlayer in solution crystals does not consist of regularly folded methylene sequences connecting adjacent crystalline sequences; such an overlayer must comprise methylene sequences randomly connecting crystalline sequences. The molecular chains forming the noncrystalline overlayer can execute local molecular motion, as suggested by T_{1C} being equal to that of the noncrystalline interzonal material in the bulk crystals, but the chain motion and the long-range conformation are restricted as shown by the very short T_{2C}.

However, an objection was raised concerning our ^1H broad-line spectrum analysis: the contribution from the noncrystalline material in the polyethylene samples should not be analyzed in terms of two components, as done in ref 1–4, but should be treated as one component.[8] Until now we were not in a position to respond to this criticism, since ^1H broad-line NMR spectroscopy is not sensitive enough to solve this problem. We report here evidence of the presence of two kinds of noncrystalline components. Moreover, we had previously no firm evidence that all of the noncrystalline components in the samples studied were detected by the above-mentioned ^1H scalar-decoupled ^{13}C NMR spectroscopy. The application of solid-state high-

0024-9297/86/2219-0636$01.50/0

Table I
Samples and Their Characterization

sample	crystallinity $(1-\lambda)_d$[a]	crystallinity $(1-\lambda)_{BL}$[b]	parameter	crystalline components: monoclinic (34.4 ppm)[c]	crystalline components: orthorhombic (33.0 ppm)[c]	noncrystalline components: interfacial (31.3 ppm)[c]	noncrystalline components: rubbery (31.0 ppm)[c]
			Bulk Crystal				
$\bar{M}_v = 3 \times 10^6$		0.620	w[d]	≈0	0.66	0.18	0.16
			$\nu_{1/2}$/Hz[e]		18	85	38
			T_{1H}/s		1.87	1.61	0.39
			T_{1C}/s		2560, 263, 1.7	0.37	0.37
			T_{2C}/ms			0.044	2.4
$\bar{M}_v = 248000$	0.761	0.755	w[d]	0.06	0.70	0.16	0.08
			$\nu_{1/2}$/Hz[e]	50	18	86	37
			T_{1H}/s		2.20	2.04	0.50
			T_{1C}/s		2750, 111, 1.3	0.41	0.41
			Solution Crystal				
$\bar{M}_v = 91000$	0.834	0.780	w[d]	0.09	0.68	0.23	≈0
			$\nu_{1/2}$/Hz[e]	60	20	133	
			T_{1H}/s		1.90	1.90	
			T_{1C}/s		220, 21, 2.0	0.46	

[a] Crystalline fractions from density measurements. [b] Crystalline fractions from ^{1}H broad-line NMR analysis. [c] Chemical shifts from Me_4Si. [d] Mass fractions. [e] Half-widths of the resonance lines.

resolution ^{13}C NMR might be expected to solve these problems. The combination of dipolar-decoupling (DD), magic-angle spinning (MAS) and cross-polarization (CP) techniques permits one to detect chemical shifts and magnetic relaxation parameters that are directly related to the chain conformation and dynamics in each phase of the structure under investigation. Indeed, in the CP/DD/MAS ^{13}C NMR spectra of polyethylene, a crystalline line corresponding to the average of the principal values of the chemical shift tensor of trans–trans methylene sequences is clearly observed.[9-11] Furthermore, an absorption line assigned to the noncrystalline methylene sequences with high molecular mobility is observed for both series of samples.[11]

The purpose of this paper is to elucidate the phase structure of lamellar polyethylene crystallized in two different ways, mainly using the differences in the longitudinal and transverse magnetic relaxation phenomena among different phases of the samples studied.

Experimental Section

Samples. A molecular weight fraction of linear polyethylene (PE) with $\bar{M}_v$ of 248 000 and an unfractionated PE with $\bar{M}_v$ of 3×10^6 were isothermally crystallized at 130 °C for 4 weeks after melting at 160 °C for 5 h and at 129 °C for 23 days after melting at 200 °C for 1 h under vacuum, respectively. A molecular weight fraction with $\bar{M}_v$ of 91 000 was isothermally crystallized at 85 °C for 24 h from 0.08% toluene solution under a nitrogen atmosphere. The viscosity-average molecular weights $\bar{M}_v$ were obtained from the relation given by Chiang.[12] The degrees of crystallinity were determined from density measurements and the broad-line proton NMR line-shape analysis as described elsewhere.[1,3] These values are listed in Table I together with the ^{13}C NMR data obtained in this work.

^{13}C NMR. ^{1}H DD/MAS ^{13}C NMR measurements were carried out at room temperature with a JEOL JNM-FX200 spectrometer operating at a field strength of 4.7 T. The radio frequency of 50.1 MHz yielding a field strength B_1 of 6.0–6.5 mT ($\gamma B_1/2\pi$ = 64.1–69.4 kHz) was used for detection of ^{13}C resonance. The ^{1}H DD field was 1.4 mT (59.5 kHz). MAS was carried out at a rate of 3.3–3.5 kHz with a bullet-type rotor made of poly(chlorotrifluoroethylene) whose volume was about 0.3 cm^3. The chemical shifts relative to tetramethylsilane (Me_4Si) were determined from the CH line (29.50 ppm[13]) of solid adamantane. The pulse sequences used are schematically shown in Figure 1. Pulse sequence I is usually used to obtain ^{13}C spectra without cross-polarization. If the waiting time τ_l after the acquisition of an FID is appropriately set, one can obtain the spectrum containing partial or total contributions from the components in the structure. Pulse sequence II was used to observe the FID under the DD condition after relaxing the transverse magnetization without ^{1}H decoupling for a given time interval τ_t. It is possible to eliminate the contribution from a rigid or less mobile component (associated with a shorter T_{2C}) by a proper choice of τ_t.

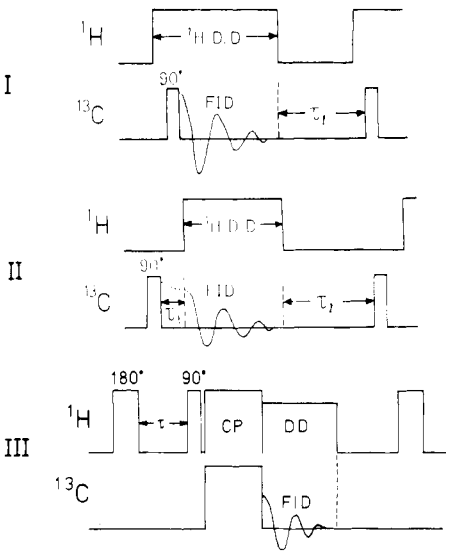

Figure 1. Pulse sequences used in this work.

The T_{1C} values longer than several tens of seconds were measured by the pulse sequence with CP developed by Torchia,[14] while the T_{1C}'s shorter than a few seconds were measured by the standard saturation–recovery pulse sequence without CP. The spin–lattice relaxation times T_{1H} of the ^{1}H magnetization were also obtained by pulse sequence III [^{H}(180°–τ–90°)–CP–^{C}(FID)], where one measures the ^{13}C magnetization that appears through the CP process after relaxation of the ^{1}H magnetization during the time τ.

Results and Discussion

A. DD/MAS ^{13}C NMR Spectra and T_{1C} Values. Figure 2 shows DD/MAS ^{13}C NMR spectra obtained by pulse sequence I for the bulk crystal with $\bar{M}_v$ of 3×10^6 (A) and the solution crystal (B). Since the τ_l's were chosen to be longer than 5 times the longest T_{1C} for each sample (see Table I), these spectra reproduce the contributions from all structural components. In the spectrum of the bulk crystal two distinct lines appear at 33 and 31 ppm. The 33 ppm value corresponds to the average of the principal values of the chemical shift tensor for trans–trans

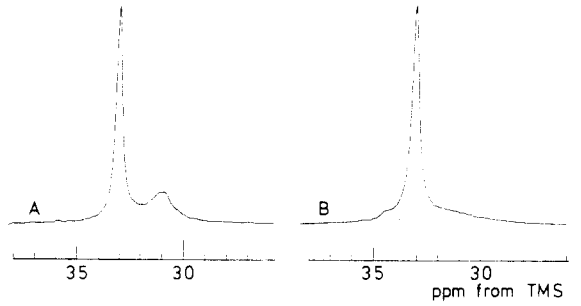

Figure 2. DD/MAS ^{13}C spectra of PE samples obtained by pulse sequence I: (A) bulk crystal with $\bar{M}_v$ of 3×10^6, $\tau_1 = 17\,000$ s; (B) solution crystal with $\bar{M}_v$ of 91 000, $\tau_1 = 1500$ s.

methylene sequences of polyethylene or *n*-paraffins in orthorhombic crystal form.[9,15,16] The 31 ppm value is close to that observed for polyethylene in solution.[17] Therefore we simply assign those lines to the crystalline and the noncrystalline components, respectively, although more detailed assignments will be given below. On the other hand, in the spectrum of the solution crystal (Figure 2B) the noncrystalline line is less resolved in comparison with the crystalline line at 33 ppm. This fact is due to the high degree of crystallinity of this sample.

In order to inquire whether each resonance line comprises a single component, we have measured T_{1C}'s by the pulse sequence developed by Torchia[14] or by the standard saturation–recovery pulse sequence. The T_{1C} values thus obtained are listed in Table I. It is seen that the crystalline component at 33 ppm has three different T_{1C}'s, 1.0–2.0, 20–260, and 220–2750 s in each sample.[18] Similar results have already been reported for different polyethylene samples,[10,19,20] although the component with the shortest T_{1C} value was incorrectly assigned as the noncrystalline component.[10] On the contrary, the noncrystalline component for all samples studied has a single T_{1C} value as short as 0.4–0.5 s, which is in good agreement with the results obtained at room temperature by ^1H scalar-decoupled ^{13}C NMR spectroscopy.[7] This indicates that the noncrystalline region is homogeneous in the relatively high-frequency molecular motion determining the T_{1C} value.

B. Detection of the Interfacial and Amorphous Noncrystalline Components. As is well-known, the relaxation of the ^{13}C magnetization of macromolecules where the only nuclei with spins are ^{13}C and ^1H predominantly arises from the time fluctuation of the dipole–dipole interaction between the ^{13}C nuclei and neighboring protons. However, the detailed mechanism of the relaxation is direction-dependent.[21] The longitudinal relaxation is attributed to the ω_C and $\omega_C \pm \omega_H$ frequency components of the fluctuation, where ω_C and ω_H denote Larmor frequencies of ^{13}C and ^1H, respectively. On the other hand, the transverse relaxation proceeds also by the contribution from the zero-frequency component of the fluctuation. Accordingly, since the transverse relaxation is sensitive to a slower molecular chain motion, different noncrystalline components can be more clearly characterized by examining this relaxation process. This holds true even in the case when the components have the same T_{1C} values as a result of the equivalent high-frequency chain motion.

^{13}C chemical shifts and the resonance line shapes, which depend on the relatively slower motion, are also very sensitive to the differences in the structure of the noncrystalline region. Moreover, ^1H spin diffusion can be utilized in discriminating the interfacial noncrystalline component from the amorphous component with rubberlike molecular mobility. Next we detect the interfacial and

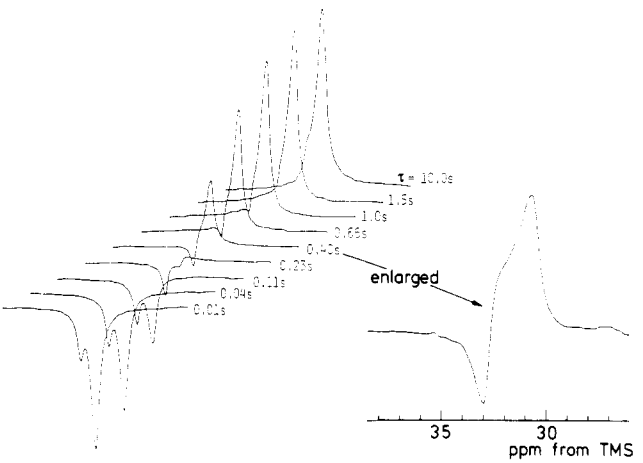

Figure 3. Partially relaxed spectra of the bulk crystal with $\bar{M}_v$ of 3×10^6, taken by inversion–recovery pulse sequence $(180°-\tau-90°-10\text{ s})_{120}$ with different τ's.

amorphous components in the three procedures, taking into account the points mentioned above.

1. Longitudinally Relaxed Spectra. Figure 3 shows the longitudinally relaxed spectra of the bulk crystal with $\bar{M}_v = 3 \times 10^6$ measured by the inversion–recovery pulse sequence $(\pi-\tau-\pi/2-10\text{ s})_{120}$ with varying τ values. The waiting time after the $\pi/2$ pulse was set to 10 s in this case. Hence, the contributions from the crystalline components with T_{1C}'s of 263 and 2560 s are eliminated due to the lack of time for recovery of the respective magnetizations. Therefore, we can observe the relaxation process of the noncrystalline line at 31 ppm in the partially relaxed spectra more clearly. For example, see the spectrum taken at $\pi = 0.40$ s, an enlargement of which is shown at the right side of Figure 3. The 33 ppm line is still in the negative z direction, while the 31 ppm line has already appeared in the positive z direction. It should be noted here that a downfield shoulder is visible on the 31 ppm line. This suggests the presence of another noncrystalline line with a different chemical shift, which will be later assigned to the interfacial component. Thus, it is evident that the bulk crystal contains two noncrystalline components with different chemical shifts and almost the same T_{1C}'s.

As far as the solution crystal is concerned, no particular relaxation phenomenon implying the presence of multiple noncrystalline components was detected by the procedure used for the bulk crystal.

2. Transverse Relaxation. Figure 4 shows stacked spectra for the bulk crystal with $\bar{M}_v$ of 3.0×10^6 obtained by pulse sequence II with $\tau_1 = 3.5$ s and different values of τ_t. Here, the contributions from the crystalline components with the T_{1C} values of 263 and 2560 s are eliminated because of the short values of τ_1. The spectrum taken with $\tau_t = 0.5$ μs is assumed to contain all noncrystalline components and a part of the crystalline component with $T_{1C} = 1.7$ s. It is seen that with increasing τ_t the contributions from the crystalline and noncrystalline components with shorter transverse relaxation times rapidly disappear, leaving only the contribution from the noncrystalline component with a longer transverse relaxation time. Thus, at $\tau_t = 100$ μs only a single peak remains at 31.0 ppm. With a further increase of τ_t, this single line gradually decreases in intensity, whereas the line shape remains essentially unchanged except for a slight narrowing. It should be noted here that the single line is closely approximated by a Lorentzian distribution function in each spectrum and that the peak position remains at 31.0 ppm in spite of the slight narrowing of the line width. Therefore, this line can be assigned to the amorphous non-

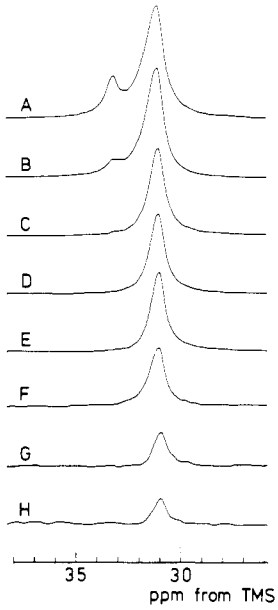

Figure 4. Partially relaxed spectra of the bulk crystal with $\bar{M}_v$ of 3×10^6, measured by pulse sequence II with $\tau_l = 3.5$ s. The τ_t's are (A) 0.5, (B) 20, (C) 60, (D) 100, (E) 140, (F) 500, (G) 2000, and (H) 4000 μs.

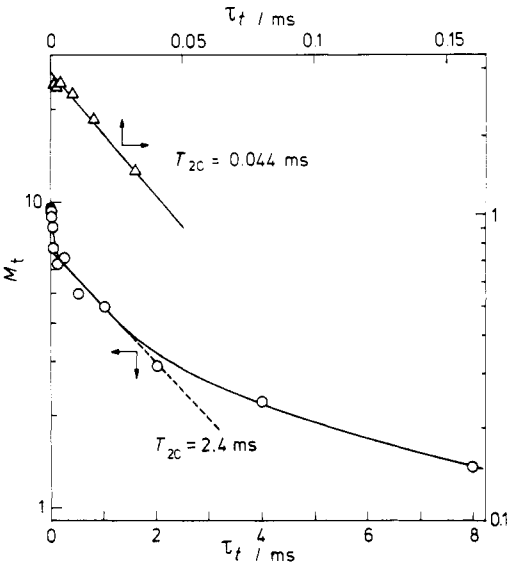

Figure 5. The 31 ppm peak height as a function of τ_t's. This peak occurs in the spectra shown in Figure 4.

crystalline component with the rubberlike, pronounced chain motion.

Figure 5 shows the semilogarithmic plot of the peak height of the line at 31 ppm pictured in Figure 4 as a function of τ_t. The overall decay curve (the bottom line in Figure 5) can be clearly resolved into two parts, a rapid decay within 50 μs and a subsequent slow decay. The initial slope of the slower decay yields $T_{2C} = 2.4$ ms, and the T_{2C} of the rapid decay has been estimated to be 44 μs by the usual decay analysis as shown at the top of Figure 5. Such an analysis of the decay curve into two components with different T_{2C}'s is more plausible than simply introducing a wide distribution of relaxation times because the T_{2C} values thus obtained differ by a factor of about 50. These two decays do not contain any contribution from the crystalline component, because the superposition of the crystalline 33 ppm line on the line at 31 ppm is negligibly small even in the spectra taken with short τ_t values (cf. Figure 4). It has therefore been confirmed that there exists two noncrystalline components with very different T_{2C} values. The component with $T_{2C} = 2.4$ ms is recognized as the amorphous component that appears as a single Lorentzian line in Figure 4. The other component, with $T_{2C} = 44$ μs, is much less mobile than the amorphous component. Therefore, this component can be assigned to the interfacial noncrystalline component in consideration of the lamellar structure of this sample and also ^{1}H spin diffusion, as shown later.

It should be pointed out here that the large deviation of the slower decay from a straight line does not indicate the existence of multiple components whose respective decays are described as single exponentials. The reason is that even in the molten state of polyethylene the ^{13}C transverse relaxation does not follow a simple exponential decay.[22] A similar nonexponential ^{1}H transverse relaxation was also observed in the same system.[23] In such a viscous system, the time scale required for the measurement of the transverse relaxation is very short in comparison with that for the time fluctuation of the local magnetic field that causes this relaxation. This may be the origin of the observed nonexponentiality of the transverse decay. It is therefore concluded that the slower decay characterizes the meltlike or rubberlike amorphous noncrystalline component, as assigned above.

Figure 6 shows the partially relaxed spectra of the solution crystal obtained in the same way as for the bulk crystal by pulse sequence II with $\tau_l = 3.5$ s and varying values of τ_t. Since the contributions from the crystalline components with the T_{1C} values of 21 and 220 s are removed from these spectra, the noncrystalline line is clearly recognized at 31.3 ppm. In contrast to the case of the bulk crystal, both absorption lines at 33 and 31.3 ppm rapidly disappear with increasing τ_t without leaving any noncrystalline component with longer T_{2C} at 31.0 ppm. See, for example, the spectrum taken with $\tau_t = 140$ μs. Even if it is enlarged 16 times, only a broad line centered around 31.3 ppm is recognized. There is no narrow line corresponding to the noncrystalline line at 31.0 ppm observed for the bulk crystal (see Figure 4D–H). It is therefore concluded that the noncrystalline region of the solution crystal is composed of a monophase of less mobile chains that have a somewhat trans-rich chain conformation as suggested by the higher chemical shift.[24]

3. ^{1}H Spin Diffusion. We have measured T_{1H}'s by pulse sequence III to determine whether ^{1}H spin diffusion occurs between the respective components that were detected in the previous sections. The T_{1H} values obtained are listed in Table I. Only one T_{1H} has been obtained for the 33.0 ppm line in each sample, although the line has three different T_{1C} values. This indicates that the proton spins rapidly diffuse throughout the crystalline region, resulting in averaged T_{1H} values. On the other hand, the noncrystalline 31.3 and 31.0 ppm lines of the bulk crystals evidently have different values of T_{1H}, indicating that spin diffusion does not significantly occur between these two components. This fact provides evidence that the noncrystalline region in the bulk crystals comprises two separate phases that cannot exchange their ^{1}H spins, probably due to the significant difference in molecular mobility. Moreover, it should be noted that T_{1H} of the 31.3 ppm noncrystalline line is very close to that of the 33.0 ppm crystalline line. This means that there is a significant ^{1}H spin diffusion between these two components. This fact verifies directly the assignment of the 31.3 ppm noncrystalline line to the crystalline–amorphous interphase.

In relation to the solution crystal as is shown in the table, the same T_{1H} of 1.90 s is obtained for both the crystalline

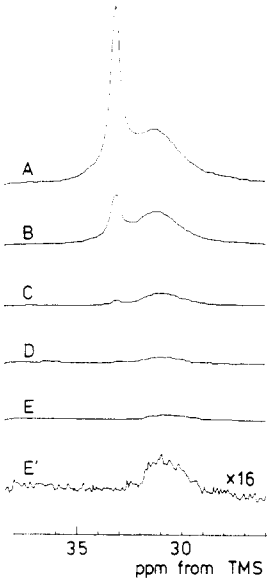

Figure 6. Partially relaxed spectra of the solution crystal taken by pulse sequence II with τ_l = 3.5 s. The values of τ_t are (A) 0.5, (B) 20, (C) 60, (D) 100, (E) 140, and (E') 140 μs. The last spectrum is enlarged 16 times.

and the noncrystalline 31.3 ppm lines, suggesting enhanced ^{1}H spin diffusion between the two components. This provides direct evidence that the noncrystalline phase forms a crystallite overlayer with restricted molecular mobility.

C. Line-Shape Analysis. As has been shown in the foregoing sections, the crystalline region comprises three components with different T_{1C} values in both bulk crystal and solution crystal. On the other hand, the noncrystalline region consists of two phases with different molecular mobilities in the bulk crystal, whereas it forms a single phase with relatively low mobility in the solution crystal. We analyze the total spectra shown in Figure 2 in terms of the contributions of these components in order to determine the mass fractions.

To this end, we have first determined the line shape of the interfacial component centered at 31.3 ppm by the subtraction of spectra; the procedure is shown in Figure 7. Here, spectrum A (the same as shown in Figure 4A) represents the contributions from all noncrystalline components and a minor contribution from the crystalline component with T_{1C} = 1.7 s. When the rubbery noncrystalline component (spectrum B; the same as shown in Figure 4E) is subtracted from spectrum A, spectrum C of the interfacial noncrystalline component can be obtained. Since this difference spectrum may be resolved by computer into two Lorentzians, the line shape of the interfacial component can be assumed to be a Lorentzian centered at 31.3 ppm. From this result, spectrum A has been analyzed in terms of three Lorentzians by least-squares fitting; the line width and the peak height of each component have been varied while keeping the peak positions of 33.0, 31.3, and 31.0 ppm constant. It is seen in Figure 7C that the curve composed of the three Lorentzians agrees well with the observed spectrum.

The total spectrum containing all the components has been analyzed in terms of three Lorentzians centered at 33.0, 31.3, and 31.0 ppm on the basis of results obtained for the short T_{1C} components. Although the crystalline line at 33.0 ppm comprises three components with different T_{1C}'s, the line has been assumed to be a single Lorentzian. The result is shown in Figure 8, where the integrated intensity fractions of the respective components

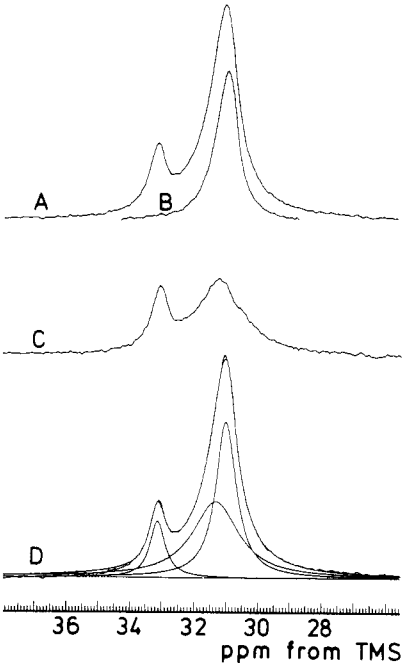

Figure 7. Analysis of the spectrum of the bulk crystal with $\bar{M}_v$ of 3 × 10^6. A and B correspond to A and E in Figure 4, respectively, C is the difference spectrum (A − B), and D is the spectrum analysis.

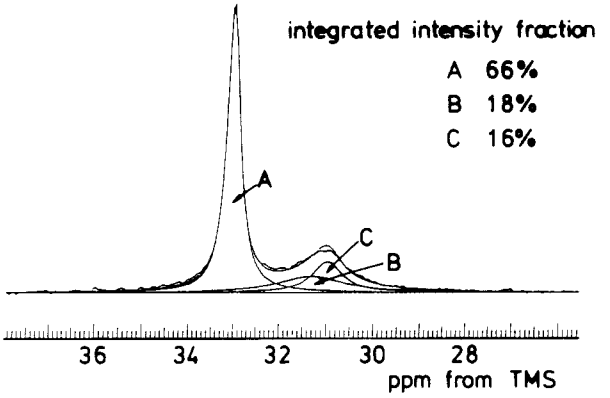

Figure 8. Component analysis of the total spectrum shown in Figure 2A. This spectrum represents the contribution from all components of the bulk crystal with $\bar{M}_v$ of 3 × 10^6: (A) crystalline component at 33.0 ppm; (B) interfacial component at 31.3 ppm; (C) rubbery component at 31.0 ppm.

are also shown. It is seen that the composite curve indicated by a dotted line reproduces well the observed spectrum. The integrated intensity fraction of the crystalline line is in good accord with the degree of crystallinity estimated by the ^{1}H broad-line NMR analysis; the latter also coincides with the value obtained from density measurements.[1-4] Therefore, this result reconfirms the assignments of the 33.0 ppm line to the crystalline component and the 31.3 and 31.0 ppm lines to the noncrystalline components.

A similar line-shape analysis was performed for the bulk crystal with $\bar{M}_v$ = 248 000. In this sample an additional crystalline line appears at 34.4 ppm that is assignable to trans–trans methylene sequences in the monoclinic crystal form.[25,26] Therefore, the spectrum was analyzed in terms of four Lorentzians with different peak positions and line widths for two crystalline and two noncrystalline lines. Reasonable curve fitting was obtained also in this case. The mass fractions and line widths of the respective components are summarized in Table I together with the T_{1C} and T_{1H} values. It is evident that this bulk crystal has a

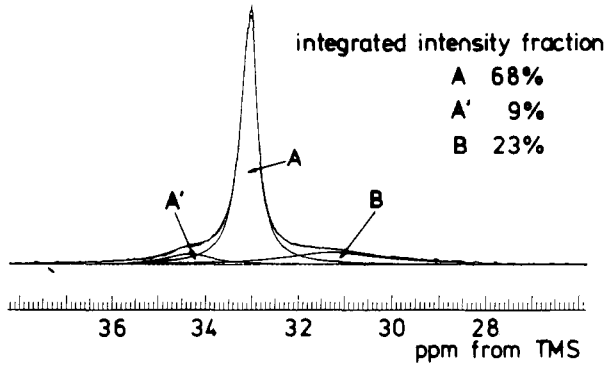

Figure 9. Component analysis of the total spectrum of the solution crystal shown in Figure 2B: (A) crystalline component at 33.0 ppm (orthorhombic crystals); (A') crystalline component at 34.4 ppm (monoclinic crystals); (B) noncrystalline component at 31.3 ppm.

similar morphological structure, containing two different noncrystalline components, to that of the bulk crystal with $\bar{M}_v = 3 \times 10^6$ except for the existence of a small amount of monoclinic crystals in the former.

Figure 9 shows the result of a line-shape analysis for the solution crystal. Since the monoclinic crystalline line is also recognized at the same position (34.3 ppm) as for the bulk crystal with $\bar{M}_v = 248\,000$,[26] the spectrum has been analyzed in terms of three Lorentzians for two crystalline and one noncrystalline lines. The composite curve of the three components is in good agreement with the observed spectrum. In this case the total fractions of the crystalline components coincide well with the degrees of crystallinity determined by other methods.

D. Phase Structure. 1. Bulk Crystals. In Figure 10 the mass fractions of the crystalline, interfacial, and rubbery components are plotted against molecular weights together with the corresponding data obtained by ^{1}H broad-line line-shape analysis.[1,3] It is evident that the results of the ^{13}C NMR analysis agree well with the results of the ^{1}H broad-line analysis. We have shown above that the ^{13}C NMR spectra can be unambiguously resolved into these components with the differences in chemical shifts and spin relaxation rates. It is therefore concluded that the ^{1}H broad-line line-shape analysis is also a reasonable method to resolve the ^{1}H spectra into its components. As a result, the previous discussion[1-4] of the phase structure of the polyethylene samples is also applicable to the results obtained in this work.

As can be seen in Figure 10, the rubbery component is negligibly small in the samples with $\bar{M}_v < 30\,000$, where the average ratio ζ_c/x of the lamellar crystal thickness to the extended molecular chain length is more than about $^1/_4$. Most of the noncrystalline region must be composed of short methylene sequences. The mobility of such short sequences is thought to be much restricted by the crystalline region, resulting in the absence of the rubbery component with liquidlike mobility. However, with further increase of molecular weight the rubbery component appears together with a pronounced decrease in the degree of crystallinity. Since the ζ_c/x value decreases substantially, molecular chains penetrate several lamellar crystallites or participate repeatedly in the same crystallites. This fact and the concomitant decrease in crystallinity may release a part of the noncrystalline component from the restriction caused by the crystalline region. As a result, the rubbery component will appear in the center of the noncrystalline region.

We have estimated the thickness ζ_i of the interfacial

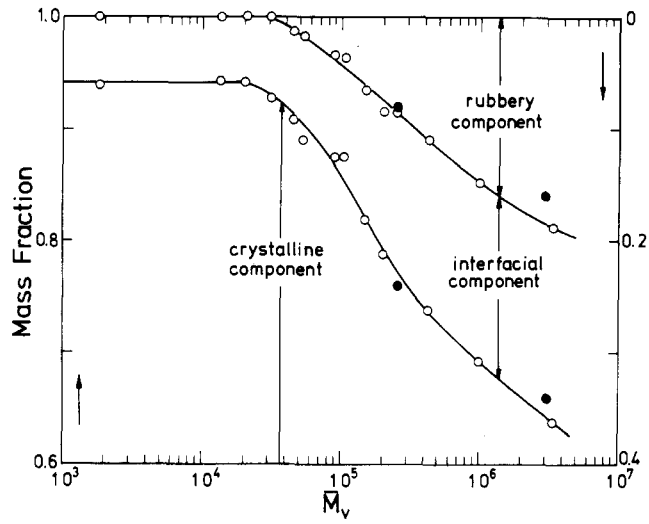

Figure 10. Mass fractions of crystalline, interfacial, and rubbery components of bulk crystals as a function of molecular weight $\bar{M}_v$: (●) ^{13}C NMR analysis (this work); (○) ^{1}H NMR analysis (ref 3).

phase by the following equation assuming the lamellar structure:

$$\zeta_i = \zeta_c x_i / 2x_c \quad (1)$$

where x_c and x_i are the fractions of the crystalline and interfacial components, respectively. In this calculation we used the ζ_c values obtained by Voigt-Martin and Mandelkern[27] and Bassett et al.[28] for linear polyethylene samples crystallized under almost the same conditions as ours. It has been found that ζ_i is about 34 Å for the bulk crystals with molecular weights of 20 000–110 000. This value corresponds closely to the thickness (15–20 Å) of the crystalline–amorphous interphase that was deduced by Flory et al. from their theoretical calculation based on the lattice model[29] as well as from the analysis of the small-angle neutron scattering results.[30,31] For higher molecular weights, the thicknesses become larger and tend to approach an asymptotic value of about 80 Å for samples with molecular weights over 10^6. Such a thick interface may be partly due to the overestimation of the lamellar sizes, which were approximately estimated from the data reported by others. In particular, thinner crystallites that are produced during gradual cooling after the isothermal crystallization at 129 or 130 °C are also of great importance in the critical characterization of the interphase. We plan to determine the lamellar sizes by the direct electron microscope observation using such a method as permanganic etching.[32]

Mandelkern and others[33,34] recently reported, based on the method developed by Strobl and Hagedorn,[35] that the semicrystalline structure of polyethylene can be analyzed in terms of crystalline, interfacial, and liquidlike amorphous components by Raman spectroscopy. However, they found that as much as 20% or more of liquidlike component is involved, even in solution crystals,[34] whereas our ^{13}C NMR analysis indicates that the crystallite overlayer is not composed of such a mobile component but of the interfacial component with restricted molecular mobility. This disagreement may arise from inconsistency of the assignments of the interfacial and amorphous components by the two spectroscopies. We are planning to make a careful comparison of the two analyses using the same polyethylene samples.

In the ^{1}H broad-line analysis[1-4] the crystalline contribution was analyzed in terms of a single component with

the line shape of the rigid orthorhombic crystal, although the contribution from the mobile crystal was also considered above 60 °C with the line shape of the n-$C_{32}H_{66}$ in the so-called C phase.[4] However, the ^{13}C NMR analysis clearly shows the presence of three or four components in the crystalline region even at room temperature. Of these, three components at 33.0 ppm have the orthorhombic crystal form and the other at 34.3 ppm the monoclinic crystal form. Although the origins of the former three components, which are discriminated by differences in T_{1C}, are not clear at present, molecular motions such as a 90° or 180° jump rotation recognized for n-paraffins[36,37] may be associated with the shorter T_{1C} components.

2. Solution Crystals. As for the bulk crystals, the characteristic phase structure of the solution crystals that was revealed by ^1H broad-line analysis has been confirmed in this work. These crystals are composed of about 80% lamellar crystallites and about 20% noncrystalline overlayers without a significant amount of a rubbery amorphous component. This structure is assumed to be essentially unaltered by changing the molecular weight of the crystal in the range 17 600–3.4×10^6.[2,3] Similar invariances have been reported in the macroscopic density[38] and in thermodynamic quantities[39] such as the interfacial free energy and the dissolution temperature. (Note, however, the large molecular weight dependence of the bulk crystals in Figure 10.) Such semiinvariance of the phase structure of the solution crystals with molecular weight is fairly consistent with small-angle neutron scattering results[40] indicating that the radius of gyration is practically independent of $\bar{M}_w$.

On the basis of the latter result, Sadler and Keller[40] proposed a "superfolding model" in which the folding of the chain is not confined to a single layer of the (110) plane; rather, the chain continues to be folded in an adjoining layer. Adjacent reentry was assumed to be the favored entity in each layer. However, Yoon and Flory[41] calculated scattering functions for superfolding models and obtained optimum agreement with experimental results when the adjacent stem arrangement in the superfolding model was diluted by a factor of 2–3 in each plane. They concluded that crystalline stems of a given molecular chain occur at small distances but are seldom adjacent to one another in the growth plane.

Our ^1H and ^{13}C NMR results for the structure of the overlayers support their conclusion. There exists no long loop that contributes to the rubbery component. On the other hand, the local molecular mobility of the overlayers is almost equivalent to that of the rubbery component contained in the bulk crystals. However, the average chemical shift (31.3 ppm) is not very different from the value (31.0 ppm) of the rubbery component. This indicates that the relatively long-range mobility of the overlayers is also rather high, although it is evidently lower than that of the rubbery component, as is seen from the difference in T_{2C}'s. Therefore, the length of the loops is not very short compared to the value of 4.5 Å required for adjacent reentry. Abe et al.[42] calculated the distribution of distances of reentry for polyethylene chain folds with 15 C–C bonds corresponding to the 80–90% crystallinity normally observed in solution crystals of polyethylene. Their conclusion that the reentry at distances less than 6 Å is highly disfavored is in good agreement with our results.

Finally, it should be noted here that the solution crystal contains an appreciable amount of monoclinic crystals whose resonance line appears at 34.4 ppm. Although the origin of this crystal form is not clear at present, it may be produced during drying of the sample. However, it is thought that the characteristic phase structure of the solution crystals is not significantly affected by the presence of monoclinic crystals.

Conclusions

The characteristic phase structure of semicrystalline polyethylene with a lamellar structure has been elucidated by the ^{13}C solid-state NMR as being composed of a lamellar crystallites, a crystalline–amorphous interface, and an isotropic amorphous phase as specified below.

(1) It is found by examining the partially relaxed ^{13}C NMR spectra in the longitudinal and transverse directions that the absorption spectra of polyethylene samples crystallized from the melt consist of crystalline lines at 33.0 and 34.4 ppm from Me_4Si. These lines are assignable to the orthorhombic and monoclinic crystal forms, respectively. Moreover, there are two noncrystalline lines at 31.3 and 31.0 ppm.

(2) The noncrystalline 31.0 ppm line represents a well-separated liquidlike amorphous phase in the structure; this assignment is based on the fact that the chemical shift is close to that observed for this polymer in solution and associated with T_{2C} as long as 2.4 ms and with T_{1H} distinctly different from that of the other noncrystalline line at 31.3 ppm.

(3) The noncrystalline 31.3 ppm line represents the crystalline–amorphous interface with a trans-rich chain conformation with restricted chain motion. This conclusion follows from the value of the chemical shift and the very short T_{2C} of the order of 0.044 ms. A T_{1H} value close to that of the crystalline 33.0 ppm line provides evidence that this line is contributed by the structural component directly adjacent to the lamellar crystallites.

(4) The 31.3 ppm line has a T_{1C} of about 0.4 s, equal to that of the 31.0 ppm line, although the T_{2C} of the former is much shorter. This leads to the conclusion that the crystalline–amorphous interface involves molecular chain motion equivalent to that occurring in the liquidlike amorphous phase as long as we are concerned with local chain motion in the frequency range corresponding to the Larmor frequencies of ^{13}C or ^1H.

(5) For samples crystallized from dilute solution only one noncrystalline line could be recognized at 31.3 ppm in addition to the two crystalline lines at 33.0 and 34.4 ppm. The character of this 31.3 ppm line resembles that of the 31.3 ppm line that is assigned to the crystalline–amorphous interface in the bulk crystals. It is concluded accordingly that solution crystals are generally composed of lamellar crystallites and interfacial overlayers without any appreciable amount of liquidlike amorphous component.

(6) The molecular chain conformation in the overlayers is quite restricted, as revealed by the substantial width and the short T_{2C} of the 31.3 ppm line. However, since T_{1C} is as long as about 0.5 s, roughly equivalent to that of the liquidlike amorphous component in the bulk crystals, it is concluded that the chain conformation in the overlayers is not as restricted as suggested by the regularly folded reentry of the molecular chain in the adjacent crystalline sequences of the same (110) plane.

Acknowledgment. We thank Dr. Barbara Gabryś, Department of Chemical Engineering and Chemical Technology, Imperial College, for valuable comments.

Registry No. Polyethylene (homopolymer), 9002-88-4.

References and Notes

(1) Kitamura, R.; Horii, F.; Hyon, S.-H. *J. Polym. Sci., Polym. Phys. Ed.* **1977**, *15*, 821.
(2) Horii, F.; Kitamaru, R. *J. Polym. Sci., Polym. Phys. Ed.* **1978**, *16*, 265.
(3) Kitamaru, R.; Horii, F. *Adv. Polym. Sci.* **1978**, *26*, 137.

(4) Horii, F.; Kitamaru, R. *J. Polym. Sci., Polym. Phys. Ed.* **1981**, *19*, 109.
(5) Bergmann, K. *J. Polym. Sci., Polym. Phys. Ed.* **1978**, *16*, 1611.
(6) Komoroski, R. A.; Maxfield, J.; Sakaguchi, F.; Mandelkern, L. *Macromolecules* **1977**, *10*, 550.
(7) Horii, F.; Murayama, K.; Kitamaru, R. *Polym. Prepr. (Am. Chem. Soc., Div. Polym. Chem.)* **1983**, *24* (2), 384.
(8) Pranadi, H.; Manuel, A. J. *Polymer* **1980**, *21*, 303.
(9) Earl, W. L.; VanderHart, D. L. *Macromolecules* **1979**, *12*, 762.
(10) Schröter, B.; Posern, A. *Makromol. Chem., Rapid Commun.* **1982**, *3*, 623.
(11) Kitamaru, R.; Horii, F.; Murayama, K. *Polym. Bull. (Berlin)* **1982**, *7*, 583.
(12) Chiang, R. *J. Polym. Sci.* **1959**, *36*, 91.
(13) Earl, W. L.; VanderHart, D. L. *J. Magn. Reson.* **1982**, *48*, 35.
(14) Torchia, D. A. *J. Magn. Reson.* **1978**, *30*, 613.
(15) VanderHart, D. L. *J. Chem. Phys.* **1976**, *64*, 830.
(16) Opella, S. J.; Waugh, J. S. *J. Chem. Phys.* **1977**, *66*, 4919.
(17) Hama, T.; Suzuki, T.; Kosaka, K. *Kobunshi Ronbunshu* **1975**, *32*, 91.
(18) The shortest T_{1C} value was determined by analyzing the decay curves measured by the saturation recovery method at a pulse repetition time of 10 s in terms of two T_{1C} components, while two longer T_{1C} values were measured by Torchia's pulse sequence.[14] Since the chemical shift of the shortest T_{1C} component is the same (33.0 ppm) as those of longer T_{1C} components, this component is thought to maintain an orthorhombic crystal form despite significant molecular mobility. The previous assignment[10] to the noncrystalline component must be revised, because the chemical shift of the noncrystalline component with the trans–trans conformation must differ from 33.0 ppm due to the different effect of chain packing, as in the case of the monoclinic crystal form shown in the text. Moreover, the rigid trans–trans conformation is unlikely to exist in the noncrystalline region of the isothermally crystallized samples at room temperature.
(19) Axelson, D. E. *J. Polym. Sci., Polym. Phys. Ed.* **1982**, *20*, 1427.
(20) Axelson, D. E.; Mandelkern, L.; Popli, R.; Mathien, P. *J. Polym. Sci., Polym. Phys. Ed.* **1983**, *21*, 2319.
(21) See, for example: Kitamaru, R., In "Stereochemical Applications of NMR Spectroscopy"; Takeuchi, Y., Marchand, P., Eds.; Verlag Chemie International: Deerfield Beach, FL, in press.
(22) Murayama, K.; Horii, F.; Kitamaru, R., unpublished data.
(23) Horii, F.; Kitamaru, R.; Suzuki, T. *J. Polym. Sci., Polym. Lett. Ed.* **1977**, *15*, 65 and related references therein.
(24) According to the method of Earl and VanderHart,[9] the fractions of gauche bonds were estimated to be 0.33 for the 31.0 ppm component and 0.38 for the 31.3 ppm component, respectively.
(25) VanderHart, D. L.; Khoury, F. *Polymer* **1984**, *25*, 1589.
(26) Relatively weak (001) diffraction of the monoclinic crystal form has been observed on the wide-angle X-ray diffraction pattern for the bulk crystal with $\bar{M}_v$ = 248 000 as well as for the solution crystal.
(27) Voigt-Martin, I. G.; Mandelkern, L. *J. Polym. Sci., Polym. Phys. Ed.* **1981**, *19*, 1769.
(28) Bassett, D. C.; Hodge, A. M.; Olley, R. H. *Proc. R. Soc. London, A* **1981**, *No. 377*, 39.
(29) Flory, P. J.; Yoon, D. Y.; Dill, K. A. *Macromolecules* **1984**, *17*, 862.
(30) Flory, P. J.; Yoon, D. Y. *Nature (London)* **1978**, *272*, 226.
(31) Yoon, D. Y. *J. Appl. Crystallogr.* **1978**, *11*, 531.
(32) Olley, R. H.; Hodge, A. M.; Bassett, D. C. *J. Polym. Sci., Polym. Phys. Ed.* **1979**, *17*, 627.
(33) Glotin, M.; Mandelkern, L. *Colloid Polym. Sci.* **1982**, *260*, 182.
(34) Glotin, M.; Domszy, R.; Mandelkern, L. *J. Polym. Sci., Polym. Phys. Ed.* **1983**, *21*, 285.
(35) Strobl, G. R.; Hagedorn, W. *J. Polym. Sci., Polym. Phys. Ed.* **1978**, *16*, 1181.
(36) Olf, H. G.; Peterlin, A. *J. Polym. Sci., Part A-2* **1970**, *8*, 753, 771, 791.
(37) Strobl, G. R. *J. Polym. Sci., Polym. Symp.* **1977**, *No. 59*, 121.
(38) Kitamaru, R.; Mandelkern, L. *J. Polym. Sci., Part A-2* **1970**, *8*, 2079.
(39) Jackson, J. F.; Mandelkern, L. *Macromolecules* **1968**, *1*, 546.
(40) Sadler, D. M.; Keller, A. *Science (Washington, D.C.)* **1979**, *203*, 263.
(41) Yoon, D. Y.; Flory, P. J. *Faraday Discuss. Chem. Soc.* **1979**, *68*, 288.
(42) Abe, A.; Jernigan, R. L.; Flory, P. J. *J. Am. Chem. Soc.* **1966**, *88*, 631.